

# Self-Adjuvanting TLR7/8 Agonist and Fentanyl Hapten Co-Conjugate Achieves Enhanced Protection against Fentanyl Challenge

Noah Powers,<sup>||</sup> Casey Massena,<sup>||</sup> Bethany Crouse, Mira Smith, Linda Hicks, Jay T. Evans, Shannon Miller, Marco Pravetoni, and David Burkhart\*

Cite This: *Bioconjugate Chem.* 2023, 34, 1811–1821

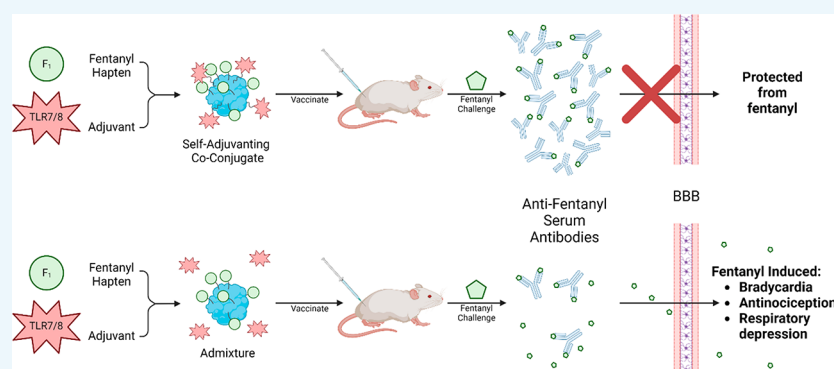
Read Online

ACCESS |

Metrics & More

Article Recommendations

Supporting Information



**ABSTRACT:** Currently approved pharmacotherapies for opioid use disorders (OUDs) and overdose reversal agents are insufficient to slow the spread of OUDs due to the proliferation of fentanyl. This is evident in the 31% rise in drug overdose deaths from 2019 to 2022, with rates increasing from 21.6 to 28.3 overdoses per 100,000 deaths. Vaccines are a potential alternative or adjunct therapy for the treatment of several substance use disorders (nicotine, cocaine) but have shown limited clinical success due to suboptimal antibody titers. In this study, we demonstrate that coconjugation of a Toll-like receptor 7/8 (TLR7/8) agonist (UM-3006) alongside a fentanyl-based hapten (F) on the surface of the carrier protein cross-reactive material 197 (CRM) significantly increased generation of high-affinity fentanyl-specific antibodies. This demonstrated enhanced protection against fentanyl challenges relative to an unconjugated (admix) adjuvant control in mice. Inclusion of aluminum hydroxide (alum) adjuvant further increased titers and enhanced protection, as determined by analysis of fentanyl concentration in serum and brain tissue. Collectively, our findings present a promising approach to enhance the efficacy of antiopioid vaccines, underscoring the need for extensive exploration of TLR7/8 agonist conjugates as a compelling strategy to combat opioid use disorders.

## INTRODUCTION

The increase in the number of opioid use disorders (OUDs) and opioid overdoses is a public health crisis which began in the 1990s and continues to grow at an alarming rate due to rapid proliferation of illicitly manufactured fentanyl and fentanyl analogues. The COVID-19 pandemic further exacerbated the incidence of OUDs and overdose in the United States, with overdose deaths increasing from 31,585 in January 2019 to 66,035 in October 2021, now representing the majority of all drug overdoses (51.41%).<sup>1,2</sup> Fentanyl and its analogues range from 3- to 10,000-fold higher potencies than morphine and have been used as adulterants for other opioids or nonopioids such as cocaine, methamphetamine, and other psychostimulants, leading to unintentional overdose.<sup>3–5</sup>

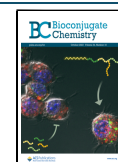
Several mu opioid receptor (MOR) agonist and antagonist medications are currently available for treating OUDs and have shown clinical utility but present several disadvantages.<sup>6</sup>

Methadone maintenance has become stigmatized, and daily visits to specialized clinics along with potentially severe side effects hinder patient compliance. Buprenorphine can be considered a safer alternative to methadone and is clinically available but requires special training and licenses. Initiation of naltrexone therapy requires individuals to abstain from opioid use for 7–14 days before treatment.<sup>7–11</sup> Additionally, patients in treatment can be at high risk for relapse and overdose due to lowered tolerance paired with tainted street mixtures.<sup>12</sup> In

Received: August 4, 2023

Revised: September 12, 2023

Published: September 27, 2023



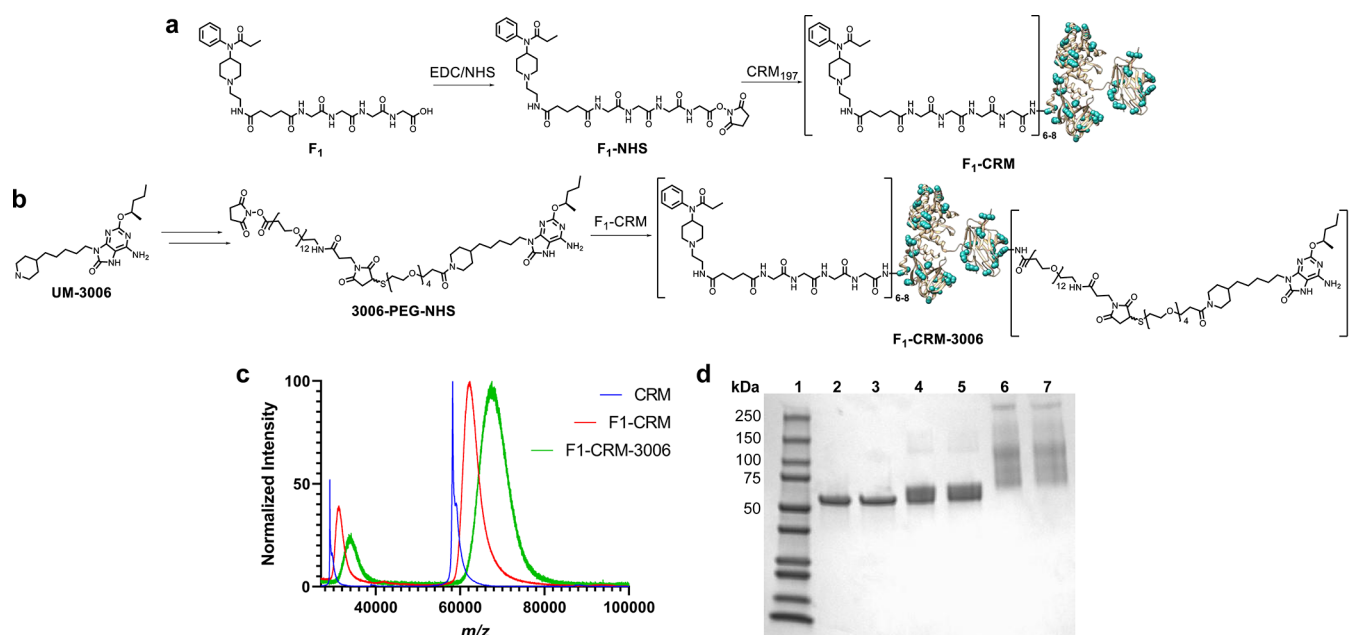


**Figure 1.** Preparation and characterization of  $F_1$ -CRM and  $F_1$ -CRM-3006 conjugates. (a) Schematic illustration of preparation of the  $F_1$ -CRM conjugate including chemical structure of  $F_1$  with a tetraglycine linker. (b) Schematic illustration of preparation of  $F_1$ -CRM-3006 including synthesis and activation of UM-3006 with PEG linkers to 3006-PEG-NHS, the active NHS ester for conjugation. (c) Representative, normalized MALDI-ToF mass spectra of CRM,  $F_1$ -CRM, and  $F_1$ -CRM-3006. Rightmost peaks  $[M + H]^+$  and leftmost peaks  $[M + 2H]^{2+}$ . (d) Image of a representative SDS-PAGE for nonreduced and reduced CRM (Lanes 2 and 3, respectively),  $F_1$ -CRM (Lanes 4 and 5, respectively), and  $F_1$ -CRM-3006 (Lanes 6 and 7, respectively). CRM structure obtained from PDB: 4AE0 and shown with lysine residues highlighted in blue.

overdose situations, MOR antagonists such as naloxone risk inadequate responses as the duration of effect of naloxone is shorter than some long-acting opioids, resulting in recurrence of respiratory depression.<sup>13</sup> Furthermore, fentanyl-induced respiratory depression could be caused in part by chest muscle rigidity known as “wooden chest syndrome”, which is mediated by cholinergic and alpha-adrenergic receptors and is not sufficiently reversed by MOR antagonists.<sup>14–16</sup>

Vaccines against fentanyl and other opioids have shown preclinical success and are proposed as an alternative or complementary strategy to traditional pharmacotherapies. These vaccines, consisting of multiple copies of opioid haptens conjugated to an immunogenic carrier protein, produce drug-specific polyclonal antibodies to sequester a drug in the serum and away from opioid receptors in the brain.<sup>17</sup> In an overdose scenario, a prophylactic intervention could be more effective than postexposure MOR antagonists which, if delayed, may not be sufficient to reverse overdose. Proof of efficacy and selectivity has been demonstrated for antioioid vaccines targeting oxycodone, heroin, fentanyl, and fentanyl analogues in a variety of preclinical models, including mice, rats, pigs, and nonhuman primates.<sup>18–21</sup> Our team has developed a lead antifentanyl hapten-carrier conjugate ( $F_1$ -CRM) which significantly reduced antinociception, respiratory depression, and brain distribution of several animal models.<sup>22</sup> The antifentanyl vaccine did not interfere with off-target opioids (methadone or naloxone) or drugs utilized in anesthesia protocols (propofol, isoflurane, atipamezole).<sup>23,24</sup> Importantly, this vaccine reduced fentanyl use in an intravenous rat self-administration model, lending validity to its use as an OUD treatment strategy as well as overdose prevention.<sup>17</sup>

Early clinical trials of nicotine and cocaine conjugate vaccines suggested insufficient antibody levels derived from highly variable patient responses that limited the efficacy of the

vaccines. Many of these vaccines solely utilized an alum adjuvant, and in those studies only ~30% of immunized subjects achieved sufficient drug-specific antibody concentrations to affect drug abstinence.<sup>12,25–27</sup> Since then, significant effort has gone into the selection of safe and potent adjuvants to increase immunity in low responders<sup>28</sup> as well as driving a more effective antibody response. Many of these adjuvants are combinations of alum and Toll-like receptor (TLR) agonists such as Monophosphoryl lipid A (TLR4), various forms of CpG ODNs (TLR9), double-stranded RNA (TLR3), and flagellin (TLR5).<sup>29,30</sup> Optimized adjuvants and delivery systems in some cases improved antioioid efficacy over alum alone while others have had mixed success,<sup>22</sup> indicating that the choice of agonist may require screening for suitability in each vaccine candidate.<sup>31,32</sup> Recently, we reported a novel lipidated TLR7/8 agonist and alum coadsorbed hapten-carrier vaccine increased fentanyl-specific antibody titers and protected against fentanyl-induced effect whereas a TLR4 agonist did not demonstrate these improved responses.<sup>22</sup> The TLR7/8 adjuvant combination also increased the Th1 polarization required to elicit fentanyl-specific IgG2a antibodies implicated in effective opioid sequestration in mice and rats.<sup>33,34</sup>

In the present study, we advanced a self-adjuvanting  $F_1$ -CRM by coconjugating a TLR7/8 alongside the  $F_1$  hapten, effectively moving the TLR agonist from the surface of alum to the surface of the carrier for more effective adjuvant delivery to antigen presenting cells (APCs) for increased immune responses while reducing off-target adjuvant toxicity.<sup>35–37</sup> Clinical development of TLR7/8 agonists as vaccine adjuvants has been slow due to the potential for rapid, systemic distribution of the small molecule after injection, leading to systemic toxicity.<sup>38–43</sup> We previously reported a modular approach to create CRM-TLR7/8 bioconjugates which

effectively increased CRM specific antibody titers as well as Th1 cytokines relative to admix controls in mice.<sup>44</sup> Here we present a bioconjugation TLR7/8 adjuvantation strategy to improve hapten-specific antibody responses. To our knowledge, this strategy has not been reported for an antiopioid vaccine, though a similar approach for polysaccharide and cancer conjugate vaccines has been pursued.<sup>45,46</sup> Our results demonstrate that coconjugation is an effective adjuvantation strategy for increasing overall titers against a small-molecule hapten. The novel TLR7/8 self-adjuvanting F<sub>1</sub>-CRM coconjugate vaccine demonstrated improved efficacy in protecting mice against fentanyl-induced antinociception, respiratory depression, and bradycardia as well as higher serum sequestration of fentanyl.

## RESULTS

### Production of F<sub>1</sub>-CRM Conjugates for Vaccines Against Fentanyl.

To perform two sequential conjugation steps (fentanyl hapten followed by TLR-7/8 adjuvant) on surface lysine residues of CRM, a new conjugation method for F<sub>1</sub> was developed (Figure 1a). While previous methods utilizing carbodiimide chemistry were effective at obtaining high haptenization ratios of F<sub>1</sub> (12–18 molar equiv to CRM), they also resulted in cross-linking of proteins, which was not conducive to coconjugation of TLR7/8 agonists in the subsequent step (Figure 1b).<sup>17,24</sup> All attempts to conjugate the TLR7/8 to F<sub>1</sub>-CRM generated by previous methods resulted in precipitation and suboptimal copy numbers. We sought to limit the extent of *in situ* O–N-migration of the 1-ethyl-3-(3-(dimethylamino)propyl)carbodiimide (EDC) activated F<sub>1</sub> carboxyl group which forms an inactive *N*-acyl urea by stabilization of the active ester with *N*-hydroxysuccinimide (NHS). Excess EDC in previous reaction mixtures, which was necessary due to being consumed by hydrolysis, likely condensed side chains and consumed primary amines of CRM limiting maximal haptenization ratio and subsequent UM-3006 copy numbers.<sup>47</sup> Addition of NHS to the EDC/F<sub>1</sub> reaction mixture prior to addition to CRM in a preactivation step allowed for EDC equivalents to be reduced while still obtaining high copies of F<sub>1</sub>. This strategy was previously reported for opioid haptens,<sup>24</sup> though its use with F<sub>1</sub> was novel. The result was a largely monomeric and homogeneous reaction product (Figure S1) which remained soluble and did not form large particulates.

Haptenization ratios for the F<sub>1</sub>-CRM conjugates were determined using matrix-assisted laser desorption ionization-time-of-flight mass spectrometry (MALDI-ToF, Figure 1c). A representative sodium dodecyl sulfate polyacrylamide gel electrophoresis (SDS-PAGE) revealed a homogeneous reaction product at approximately 60 kDa, in line with MALDI-ToF spectra. SDS-PAGE also revealed minimal cross-linking of F<sub>1</sub>-CRM as reflected by a low-intensity band at 120 kDa (Figure 1d, lanes 4 and 5). We elected to reduce CRM haptenization ratios to a target of 6–8 (previously >10) to preserve available lysine residues for subsequent coconjugation of adjuvant.

The immunogenicity of F<sub>1</sub>-CRM conjugates (without TLR7/8 adjuvant) from both the EDC and EDC/NHS conjugation methods was tested in mice at two doses (1 and 5 μg) of F<sub>1</sub>-CRM with and without alum. Unadjuvanted responses against conjugates made with the new conjugation process (EDC/NHS) showed little to no differences in F<sub>1</sub>-specific IgG antibody titers compared to those generated with

the previous conjugation process (EDC), but significantly improved responses were observed in EDC/NHS F<sub>1</sub>-CRM groups adjuvanted with alum (Figure S2a). IgG1 and IgG2a subtype titers were largely consistent with the total IgG trends, with the new conjugate providing significantly improved antibody titers in the high-dose F<sub>1</sub>-CRM groups (Figure S2b,c).

**Production of Self-Adjuvanted F<sub>1</sub>-CRM-3006 Co-Conjugate.** For the co-conjugate, we selected the TLR7/8 agonist UM-3006 (Figure 1b) which previously increased CRM specific antibody responses when conjugated to surface lysine residues.<sup>44</sup> We elected to target an average of four copies of UM-3006 per CRM, which previously increased anti-CRM responses at a CRM dose of 1 μg while retaining high process yields.<sup>44</sup> The lysine-reactive NHS ester of UM-3006 was added stepwise to F<sub>1</sub>-CRM until the desired UM-3006 copy number was obtained. Changes to molecular weight could be observed by MALDI-ToF during the reaction, allowing for real-time and accurate characterization, leading to a reproducible copy number as reactions were quenched after the target was reached. Additionally, the poly(ethylene glycol) (PEG) spacers provided a hydrophilicity reservoir for both the F<sub>1</sub>-CRM and UM-3006 components minimizing observed precipitation of the coconjugate (hereafter F<sub>1</sub>-CRM-3006), and yields after purification were high (>70%). A complete description of conjugates utilized in all subsequent studies is provided in Table S1.

A broad band was observed in the SDS-PAGE of the coconjugate (Figure 1d, Lanes 6–7) beginning at approximately 60 kDa and continuing to 150 kDa which was not corroborated by MALDI-ToF. This is not suspected to be the result of cross-linking which would result in two discrete bands as observed with F<sub>1</sub>-CRM and could be due to a known interaction between SDS and PEG resulting in altered migration properties from proteins of similar molecular weights.<sup>48</sup> Also, for complicated proteins with multiple reaction sites and several potential combinations of hapten and adjuvant copy number, SDS-PAGE has been suggested to offer poor resolution but was included for completeness.<sup>49</sup>

**Adsorption of F<sub>1</sub>-CRM, F<sub>1</sub>-CRM-3006, and UM-3006 to Alhydrogel.** Admixed vaccines (denoted with a “+” between vaccine components) were studied at 1× and 10× molar equivalent dosages of UM-3006 relative to the coconjugate adjuvant dose while holding the dose of F<sub>1</sub>-CRM constant at 1 μg of the CRM carrier. Based on previous studies in which alum further enhanced hapten-specific antibody titers we also chose to include alum here.<sup>22</sup> Recovery of UM-3006 in the supernatant after centrifugation confirmed minimal adsorption of this adjuvant to the surface of alhydrogel at either 1× (27%) or 10× doses (2%). No F<sub>1</sub>-CRM or F<sub>1</sub>-CRM-3006 was detected in the supernatant of samples containing alum indicating adsorption of the F<sub>1</sub>-CRM conjugate to the surface of alhydrogel was not disrupted by the presence of UM-3006 at either 1× or 10× doses or in conjugate form (Table S2).

**Immunogenicity of F<sub>1</sub>-CRM+UM-3006 and F<sub>1</sub>-CRM-3006 with or without Alhydrogel.** Mice were vaccinated intramuscularly (IM) in the left calf on days 0 and 14, and serum was harvested at day 28 (14 days post booster vaccination) for evaluation of humoral immunity. As evaluated by enzyme-linked immunosorbent assay (ELISA), F<sub>1</sub> specific IgG antibody titers in mice vaccinated with F<sub>1</sub>-CRM-3006+alum were significantly higher than those in all other

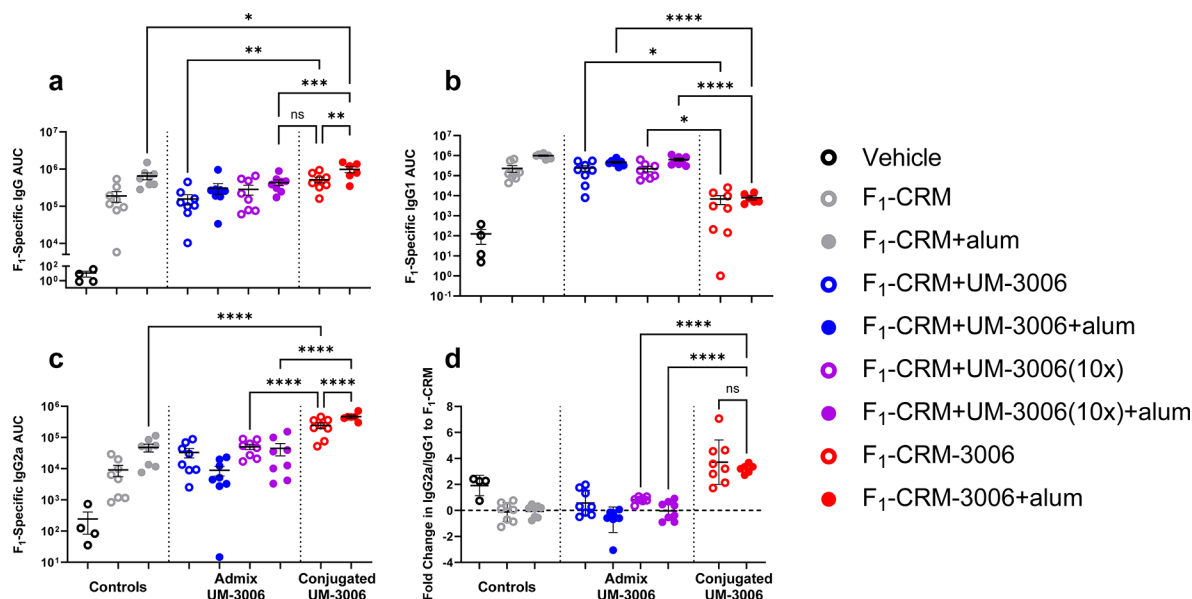


**Figure 2.** Vaccination of mice with coconjugates enhances F<sub>1</sub>-specific IgG antibody levels in sera. BALB/c mice ( $n = 6$  or  $8$  per group) were immunized with 1  $\mu$ g of CRM (1.06  $\mu$ g F<sub>1</sub>-CRM) on days 0 and 14, and serum was harvested on day 28. Vaccines were adjuvanted with UM-3006 as coconjugates and 1X or 10X molar dose admixtures. Select groups also included alum. F<sub>1</sub>-specific serum (a) total IgG, (b) IgG1, and (c) IgG2a titers were determined by ELISA on day 28. (d) Log of fold change in IgG2a and IgG1 to F<sub>1</sub>-CRM ratios to examine changes in Th1/Th2 polarization. Data are expressed as mean  $\pm$  SEM. Brackets indicate select pairwise group comparisons using one-way ANOVA followed by Fisher's LSD test. Symbols: \* $p \leq 0.05$ , \*\* $p \leq 0.01$ , \*\*\* $p \leq 0.001$ , and \*\*\*\* $p \leq 0.0001$ .

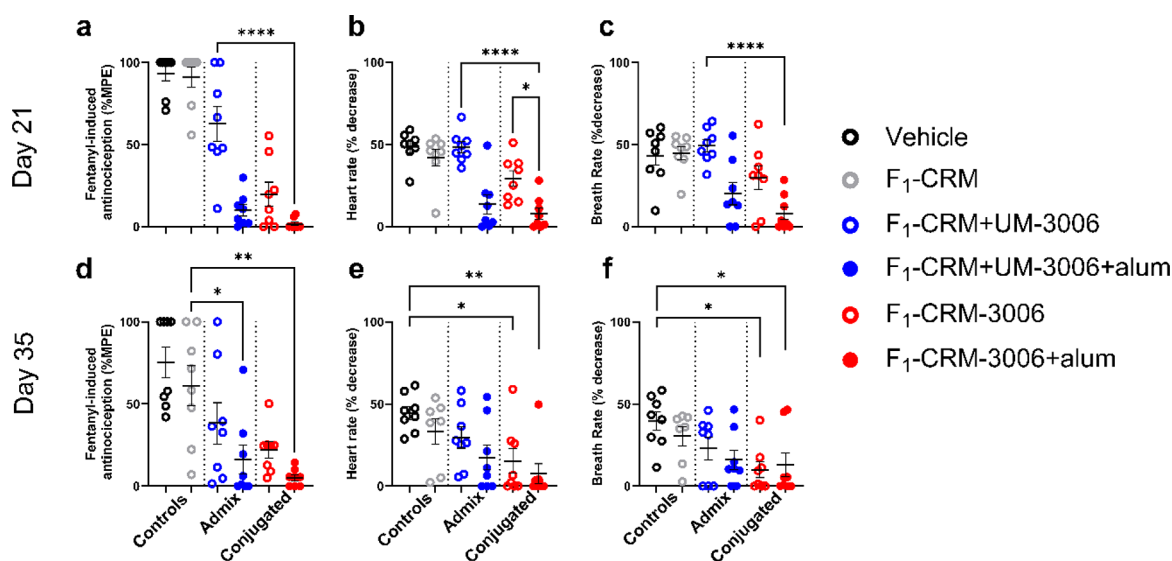


**Figure 3.** Co-conjugation protects against the fentanyl challenge in mice. F<sub>1</sub>-CRM and F<sub>1</sub>-CRM-3006 conjugates were tested in BALB/c mice ( $n = 8$  per group) to compare dose matched UM-3006 admix and coconjugate formulations with and without alum adjuvant. Injections of 1  $\mu$ g of F<sub>1</sub>-CRM were performed on days 0, 14, and 28 with 0.05 mg/kg sc fentanyl challenge on days (A–C) 21 and (D–F) 35. Data expressed as mean  $\pm$  SEM. Brackets indicate pairwise comparisons using one-way ANOVA followed by Tukey's multiple comparisons. Symbols: \* $p \leq 0.05$ , \*\* $p \leq 0.01$ , and \*\*\*\* $p \leq 0.0001$ .

groups (Figure 2a, selected pairwise comparisons). Mice vaccinated with F<sub>1</sub>-CRM-3006 alone displayed F<sub>1</sub>-specific IgG titers significantly higher than those of the 1X admixture. This group also displayed comparable F<sub>1</sub>-specific IgG titers to the alum and 10X admixed groups, demonstrating the efficacy of this TLR7/8 adjuvant delivery system.

Titers of F<sub>1</sub> specific IgG subtype antibodies were obtained to identify differences between vaccines in their ability to drive Th1 (IgG2a) and/or Th2 (IgG1) polarization (Figure 2b,c).<sup>50–52</sup> Co-conjugate groups significantly enhanced F<sub>1</sub>-

specific IgG2a titers over admixtures and controls while simultaneously decreasing F<sub>1</sub>-specific IgG1 titers, suggesting a strongly Th1 biased T helper response.

To highlight the impact of the adjuvant on T-cell polarization, we divided titers by the mean titer of the F<sub>1</sub>-CRM group for both subtypes to obtain the fold change from an unadjuvanted control. The fold change in IgG2a was then divided by the fold change in IgG1 to obtain a fold change ratio of IgG2a to IgG1 which was log transformed. Positive values correspond to an increase in Th1 polarization, while

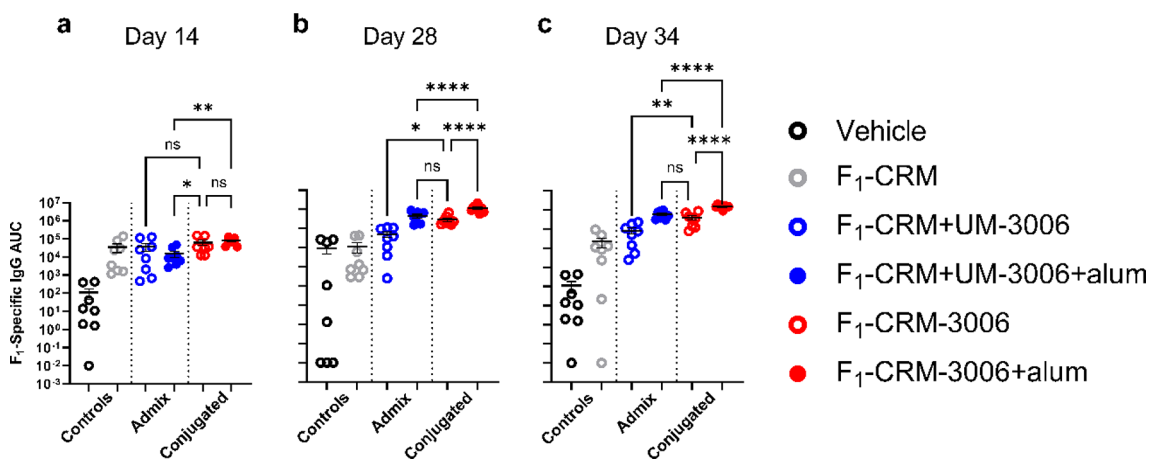


**Figure 4.** Vaccination with F<sub>1</sub>-CRM-3006 conjugates with or without alum increases serum IgG relative to the admixed control. Mice are the same as those shown in Figure 3. F<sub>1</sub>-specific IgG serum concentrations were determined on days (A) 14, (B) 28, and (C) 34. Data are expressed as mean  $\pm$  SEM. Brackets indicate pairwise group comparisons using one-way ANOVA followed by the Fisher's LSD test. Symbols: \* $p \leq 0.05$ , \*\* $p \leq 0.01$ , \*\*\*\* $p \leq 0.0001$ .

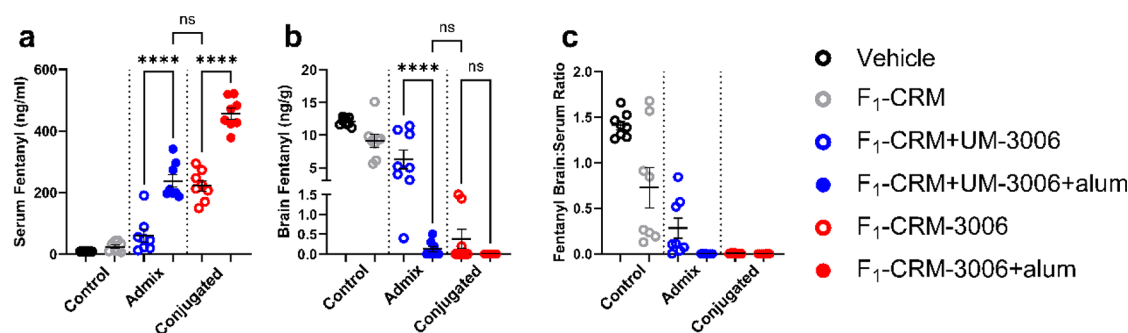


**Figure 5.** Co-conjugate vaccination significantly restricts fentanyl distribution away from the brain relative to the admixed control. Mice are the same as those shown in Figures 3 and 4 following the challenge on day 35. Fentanyl concentrations in the (A) serum and (B) brain were determined using LC-MS/MS. (C) Ratios of fentanyl in the serum and brain calculated for each mouse. Data are expressed as mean  $\pm$  SEM. Brackets indicate pairwise comparisons using one-way ANOVA followed by Tukey's multiple comparisons. Symbol: \*\*\*\* $p \leq 0.0001$ .

adjuvant formulations that did not change polarization relative to F<sub>1</sub>-CRM only are closer to zero (Figure 2d). Both groups receiving F<sub>1</sub>-CRM-3006 demonstrated a bias toward F<sub>1</sub> specific IgG2a antibodies. This bias was retained or slightly increased with codelivery of alum adjuvant which is well-known to bias immune responses toward Th2 and production of IgG1 antibodies.<sup>53</sup>

Since the conjugated UM-3006 may result in the generation of anti-UM-3006 and/or anti-PEG linker specific antibodies, an ELISA using UM-3006 conjugated to bovine serum albumin (BSA) was developed to quantify 3006- and/or PEG-specific antibody titers. UM-3006 and/or PEG linker antibodies were detected in the mice vaccinated with the coconjugate (Figure S3). However, polyclonal antibody affinities toward F<sub>1</sub> remained high and unchanged in the coconjugate groups as evaluated by Biolayer Interferometry (BLI, Figure S4a). The dissociation constants ( $k_d$ ) trended with the total IgG antibody titer (Figure S4b).

#### Fentanyl Challenge of Mice Vaccinated with F<sub>1</sub>-CRM+3006 and F<sub>1</sub>-CRM-3006 with or without Alhydrogel.

Dose matched 1 $\times$  UM-3006 admix and conjugate vaccines with and without alum were advanced into a mouse fentanyl challenge model, and the effect of vaccination on fentanyl-induced antinociception, bradycardia, and respiratory depression was determined by latency to respond on a hot plate, heart rate, and breath rate, respectively. Animal responses were

measured after two separate fentanyl challenges of 0.05 mg/kg, corresponding to 7 days postsecondary (Figure 3a-c) and 7 days post-tertiary (Figure 3d-f) vaccination with a 14-day washout between challenges. Overall, the two coconjugate groups and the admixture of UM-3006 and alum all demonstrated a significant reduction in fentanyl-induced effects compared to controls. However, no differences were detected between these three vaccines. Except for Day 35 breath rate, the F<sub>1</sub>-CRM-3006+alum vaccine group trended toward being the most protective by all metrics tested. Co-conjugate groups trended toward greater protection than their admixed counterparts, and the UM-3006 admixed with alum adjuvanted group failed to show significantly greater protection than the F<sub>1</sub>-CRM-3006 group without alum.

Mouse behavioral responses correlated with anti-F<sub>1</sub> IgG titers determined for each group on Days 28 and 34, corresponding to just prior to the first and second challenge, Days 21 and 35, respectively (Figure 4). For both challenges, F<sub>1</sub>-CRM-3006+alum demonstrated significantly higher titers than all other groups. Titers on Day 14 were measured, although many groups were unable to be differentiated until Day 28. The difference between the admixed alum group and the coconjugate was not significant on either day 28 or 34. F<sub>1</sub>-CRM-3006+alum induced a significant increase in F<sub>1</sub>-specific IgG titer relative to the admixed control. F<sub>1</sub>-specific IgG1

(Figure S5a–c) and IgG2a (Figure S5d–f) titers at days 14, 28, and 34 were also measured.

**Effect of Vaccination on Fentanyl Distribution Following Challenge.** Vaccine efficacy was also assessed by measurement of fentanyl concentration in the brain and serum following a challenge in vaccinated mice. After physiological effects from the Day 35 challenge were recorded, samples of trunk blood and brain were obtained and analyzed for fentanyl concentration using liquid chromatography-tandem mass spectrometry (LC-MS/MS). Mice vaccinated with F<sub>1</sub>-CRM-3006+alum demonstrated significantly increased retention of fentanyl in serum compared to all other groups (Figure 5a). The same group trended toward greater restriction of fentanyl away from the brain with no detectable fentanyl in the brain of any mouse in the F<sub>1</sub>-CRM-3006+alum group (Figure 5b). However, brain fentanyl concentrations in F<sub>1</sub>-CRM-3006+alum vaccinated mice were not significantly different from those of the F<sub>1</sub>-CRM-3006 group or the admixed F<sub>1</sub>-CRM+UM-3006+alum groups.

## DISCUSSION

Prophylactic or therapeutic vaccination against OUDs presents a promising alternative to reduce the risk of opioid overdose in vulnerable populations and provides alternatives to currently approved therapies for treating OUD. Co-conjugate vaccines, alone or in combination with alum, significantly increased F<sub>1</sub> specific antibodies relative to admixtures of the same components, resulting in higher efficacy following fentanyl challenge. F<sub>1</sub>-specific antibodies have been previously demonstrated to be fentanyl-specific.<sup>54</sup>

Vaccination with the F<sub>1</sub>-CRM conjugate has proven to be robust at eliciting protective antibody responses against fentanyl, sufentanil, and acetylfentanyl at varying haptenization.<sup>17,24</sup> Despite changes in synthesis, adjuvantation, and conjugation chemistry over the course of its development, F<sub>1</sub>-CRM has consistently demonstrated protection against potentially lethal fentanyl doses and reduced fentanyl use in a rat self-administration model. We have further refined the conjugation process using NHS active esters to reduce the amount of EDC necessary to obtain a relevant hapten ratio without excess cross-linking of the protein. This new conjugate allowed for coconjugation of UM-3006 to F<sub>1</sub>-CRM in a single step and purification of excess agonist without observing precipitation and retaining high yields. While conjugation of TLR7/8 agonists to antigenic proteins has been reported previously,<sup>43,44,46,55</sup> to our knowledge this is the first application of the technology to addictive drug hapten vaccines.

With this novel coconjugate developed, performance of the self-adjuvanting vaccine was directly compared to the admixed TLR7/8 adjuvant and F<sub>1</sub>-CRM controls. Our *in vivo* results demonstrate that coconjugation of the UM-3006 adjuvant to the surface of a hapten carrier protein is a more effective adjuvantation strategy than dose-matched admixtures. As UM-3006 and its PEG linker are larger than F<sub>1</sub> and its glycine linker, it was possible that the addition of this second, larger hapten might have interfered with antibody recognition of F<sub>1</sub>. However, given the dramatic increase in F<sub>1</sub>-specific antibody titers observed with coconjugation with UM-3006, this does not appear to be the case. Also, the anti-UM-3006 or PEG linker antibodies after vaccination did not appear to interfere with the production of high titer anti-F<sub>1</sub> antibodies in the coconjugation groups.

A second goal of the study was to observe the impact of including alum adjuvant with the admixed and coconjugated TLR7/8 adjuvant. We have recently reported an alternate adjuvanted F<sub>1</sub>-CRM vaccine, which demonstrated increased F<sub>1</sub>-specific antibody titers when a lipidated TLR7/8 adjuvant was combined with alum and F<sub>1</sub>-CRM.<sup>22</sup> Overall, the high F<sub>1</sub>-specific titers and *in vivo* efficacy of the coconjugate with alum here indicate this modality is also an effective adjuvant combination strategy. Addition of alum significantly enhanced titers and serum fentanyl after the challenge, although reductions in brain fentanyl levels and improvements in physiological data at a 0.05 mg/kg fentanyl dose were less apparent. For the F<sub>1</sub>-CRM-3006+alum group, the fentanyl dose appears to be below the fentanyl binding capacity these high serum antibody titers can retain since no fentanyl was detected within the brain of any mice in the group. This could also have contributed to the lack of significant differences in physiological data among the three highest titer groups of F<sub>1</sub>-CRM-3006+alum, F<sub>1</sub>-CRM-3006, and F<sub>1</sub>-CRM+3006+alum. A dose escalation study could be necessary to evaluate differences between these vaccine groups.

Overall, these data suggest coconjugation to be a more effective adjuvantation strategy to admixtures as there was no significant difference in antibody titers between the two adjuvant admixtures of 1× and 10× UM-3006 with alum and the single adjuvant F<sub>1</sub>-CRM-3006 coconjugate. However, addition of alum to the F<sub>1</sub>-CRM-3006 vaccine may still be necessary to maximize vaccine protection, as further increases in antibody titers and fentanyl serum concentration were observed. Future studies could evaluate increasing the dose of CRM and, therefore, both hapten and adjuvant dose in the coconjugate groups to potentially reduce the reliance on alum.

Additionally, the increased vaccine responses observed in the present data may have resulted from changes in the physical properties (size, molecular weight, and solubility) and not directly from the activity of the adjuvant or increases in the efficiency of adjuvant delivery. However, it should be noted the previous F<sub>1</sub>-CRM was cross-linked to the extent that very little monomer was observed by SDS-PAGE and formed large particulates which remained at the top of the wells but was demonstrated to be suboptimal *in vivo* (Figures S1–S2). Given the dramatic differences in size for the two candidates as well as the lower F<sub>1</sub> copy number for the new conjugate, this implies size minimally impacts the responses to F<sub>1</sub>-CRM. Nevertheless, a study of a mixture of conjugates (F<sub>1</sub>-CRM and CRM-3006) versus the coconjugate (F<sub>1</sub>-CRM-3006) might reveal negligible differences in responses. A CRM-3006 conjugate may inherently demonstrate an increased adjuvanticity or could distribute similarly to F<sub>1</sub>-CRM unlike the UM-3006 small-molecule admixtures reported here. Poignantly, both conjugates would be expected to adsorb to alum, limiting dissociation of UM-3006.

In comparison to previous studies, the *in vivo* experiments presented here used relatively low doses of the hapten conjugate. Opioid hapten-carrier vaccines adjuvanted with alum have previously used 25–100 μg per dose (mice and rats) with as much as 500 μg of alum adjuvant.<sup>17,56–58</sup> We recently reported that 5 μg of F<sub>1</sub>-CRM in combination with 22.5 μg of alum and 10 μg (8760 pmol) of lipidated TLR7/8 adjuvant (INI-4001) per dose was sufficient to achieve a similar result.<sup>22</sup> In this study, we furthered this dose reduction with 1 μg of CRM carrier (equivalent to 1.06 μg F<sub>1</sub>-CRM) with the same 22.5 μg of alum adjuvant in the same BALB/c mouse model.

UM-3006 dosing was restricted to a molar ratio of 4:1 adjuvant to carrier for both the admixed and coconjugate groups resulting in a TLR7/8 dose of 55.1 or 66.5 pmol (Table S1) for a single dose, a dose reduction of at least 132× versus INI-4001. This antigen- and adjuvant-sparing effect indicates improved efficacy of TLR7/8 adjuvants when coconjugated. It has been previously proposed that conjugation of several copies of adjuvant to a single carrier achieves a cluster effect within the processing APC though the relative potency of INI-4001 to UM-3006 could also contribute.<sup>46,59</sup> Studies of the coconjugate vaccine presented here against other TLR7/8 adjuvanted F<sub>1</sub>-CRM vaccine formulations should be conducted to establish which is most ideal for not only efficacy but also vaccine supply, patient safety, and compliance. Adverse events for adjuvanted vaccines are likely to be dose-dependent; however, conjugation of the TLR7/8 to a lipid or a carrier can prevent the small molecule from entering the blood causing waste inflammation.<sup>37</sup>

We also evaluated the adjuvant effects on class switching since antiopioid IgG2a has been reported to exhibit greater protection than IgG1.<sup>33</sup> Here we report that groups with the highest anti-F<sub>1</sub> IgG2a titers also exhibited the strongest protection from fentanyl challenge, providing further evidence to support this finding. Studies comparing adjuvanted vaccines, which provide high F<sub>1</sub>-specific IgG1 responses and passive immunization with opioid-specific subclasses, would provide additional support. However, since there is no currently well-supported mechanism for IgG2a effector functions to confer greater protection, it is difficult to determine whether an increase in Th1 polarization would continue to demonstrate greater protection in other animal models.<sup>60</sup>

## CONCLUSIONS

The present study focused on the coconjugation of UM-3006, a TLR7/8 agonist, with the F<sub>1</sub> fentanyl hapten to the surface of CRM. These data present coconjugation as an alternative TLR7/8 adjuvanting strategy to successfully mitigate the effects of fentanyl challenge at a lower dose of both adjuvant and F<sub>1</sub>-CRM, which could alleviate vaccine-induced side effects. The efficacy of the coconjugate vaccine demonstrated significant increases in protection versus an admix control, and this protection was improved by adsorption of the vaccine to alum. Co-administration of antigen and adjuvants is increasingly considered to be a viable vaccination strategy to create an antigen dose-sparing effect as well as potentially increasing the durability of responses across a genetically diverse population. Use of a coconjugated F<sub>1</sub>-CRM-3006 vaccine resulted in a highly Th1 polarized response, which warrants further study to observe the impact of immune bias on protection of mice as well as other OUD animal models. Furthermore, these results highlight the adaptability of the highly modular and soluble PEG cross-linking platform our group has developed which we are working to apply to other vaccine antigens to address multiple unmet medical needs.

## EXPERIMENTAL PROCEDURES

**Materials and Instrumentation.** All starting reagents and materials were purchased from commercial sources and used without further purification. For a detailed description of materials and instrumentation, please consult [Supporting Information](#).

**Synthesis and Characterization of F<sub>1</sub>-CRM and F<sub>1</sub>-BSA Conjugates.** To increase dimethylformamide (DMF) solubility, the F<sub>1</sub> lithium salt was exchanged for a trifluoroacetic acid salt. F<sub>1</sub>-Li (10.34 or 9.50 mg) was dissolved in 0.1% trifluoroacetic acid (TFA)/water (517.0 or 500.0 μL) and held at ambient temperature for 30 min. A Zeba Spin Desalting Column (7000 molecular weight cutoff (MWCO), 2 mL) previously equilibrated with 0.1%TFA/Water (3 × 500 μL) was loaded with F<sub>1</sub> and centrifuged at 1000g for 2 min. F<sub>1</sub>-TFA was then eluted with 0.1%TFA/Water. All eluent (4 mL) was collected and combined before being thoroughly desiccated. The resulting F<sub>1</sub>-TFA salt product was a white powder (13.0 mg, 107% and 15.4 mg, 138%) and stored desiccated at -20 °C.

F<sub>1</sub>-TFA was dissolved in 25% v/v dimethyl sulfoxide (DMSO)/DMF (7.04 mg, 384.8 μL, 1 equiv or 15.4 mg, 840.2 μL, 1 equiv). Dry powders of EDC·HCl (4.0 equiv) and NHS (4.0 equiv) were weighed and added directly to the reaction vial for preactivation of F<sub>1</sub>. Reactions were clear and colorless immediately after mixing. After an overnight hold at ambient temperature, reactions were clear and slightly yellow. Immediately prior to protein conjugation, the acid content of reaction mixtures was neutralized with *N,N*-diisopropylethylamine (DIPEA) (3 equiv). The mixture was then titrated into a solution of CRM or BSA (1 mg/mL, 10 mM phosphate buffer pH 7.2), waiting 30 min after each addition before determining haptenization ratios. Haptenization ratios were calculated by dividing the difference in the masses of the starting material (CRM 58400 g/mol, BSA 66500 g/mol) and reaction product (F<sub>1</sub>-CRM, Table S1 and F<sub>1</sub>-BSA, 72742 g/mol) by the mass of F<sub>1</sub> and the linker *sans* hydroxyl group (599.7 g/mol). Once the target haptenization ratio was observed (F<sub>1</sub>-CRM target 6–7, F<sub>1</sub>-BSA target >10), reactions were thoroughly purified with Amicon filters and 10 mM phosphate buffer pH 7.2. Removal of unreacted reagents was confirmed by analytical C18 reverse-phase high-performance liquid chromatography (RP-HPLC) at 210 nm (Figure S6) after which the product was sterile-filtered (Millex-GV, EMD Millipore) and stored at 2–8 °C. For the comparison of conjugation methods, F<sub>1</sub>-CRM was generated as previously reported.<sup>24</sup>

**Synthesis and Characterization of F<sub>1</sub>-CRM-3006 and BSA-3006 Conjugates.** Synthesis of 3006-PEG-NHS was conducted as previously described.<sup>44</sup> In brief, UM-3006-HCl (14.85 mg, 1 equiv) was dissolved in DMSO (594.0 μL, 25 mg/mL). To this vial, a solution of SAT(PEG)<sub>4</sub> 100 mg/mL in anhydrous DMF was added (1.2 equiv, 175.9 μL). The reaction was initiated by addition of DIPEA (3.0 equiv, 21.8 μL), and the target was isolated with preparatory-scale RP-HPLC. Removal of the thioacetate group was conducted by product in DMF (20 mg/mL) and then adding an equal volume of 1 M NH<sub>2</sub>OH·HCl in 0.2 M phosphate buffer at pH 7.2. After 30 min of gentle mixing, the target was isolated with preparatory-scale RP-HPLC and then dried overnight. 3006-PEG-NHS was then synthesized *in situ* by dissolving the deprotection product in anhydrous DMF (1 eq, 20 mg/mL) and titration of a stoichiometric amount of SM(PEG)<sub>12</sub> (50 mg/mL in anhydrous DMF) as monitored by LC/MS to confirm complete reaction of starting material. The reaction was initiated with a single addition of DIPEA (3 equiv). The reaction mixture was then held desiccated at -20 °C until conjugation.

Production of F<sub>1</sub>-CRM-3006 was conducted based on procedures previously reported for production of a CRM conjugate.<sup>44</sup> An aliquot of F<sub>1</sub>-CRM or BSA in 10 mM phosphate buffer pH 7.2 was placed into a plastic vial (1 eq, 1 mg/mL) into which the 3006-PEG-NHS *in situ* mixture was titrated. Reaction was briefly mixed and then held for 15–30 min prior to checking adjuvant copy number by MALDI-ToF. Adjuvant copy numbers were calculated by dividing the difference in the estimated masses of the starting material (BSA 66500 g/mol or F<sub>1</sub>-CRM Table S1) and reaction product (F<sub>1</sub>-CRM-3006, Table S1 and BSA-3006 85699 g/mol) by the mass of 3006-PEG *sans* NHS leaving group (1405.71 g/mol). Conjugates were thoroughly purified after reaching the target copy number (F<sub>1</sub>-CRM-3006 targeted 4, BSA-3006 targeted >10) using Amicon filters and 10 mM phosphate buffer pH 7.2. Removal of unreacted reagents was confirmed by analytical C4 or C18 RP-HPLC analysis at 280 nm (Figure S7) after which the product was sterile-filtered and stored at 2–8 °C.

**Vaccine Formulation and Alum Adsorption.** Mouse vaccinations were assembled immediately prior to injection with the indicated amounts of F<sub>1</sub>-CRM, F<sub>1</sub>-CRM-3006, alum, and/or UM-3006. Formulations were diluted with 2% glycerol in water as necessary to reach 50  $\mu$ L total volume per injection and mixed end over end for 1 h prior to injection for complete alum adsorption. Dosing of UM-3006 was standardized to the adjuvant dose of the F<sub>1</sub>-CRM-3006 lot used in each study (Table S1) with all mice receiving the same adjuvant dose (1 $\times$ ) or a 10-fold higher dose (10 $\times$ ) as indicated. UM-3006-HCl for admixed groups was prepared at 50  $\mu$ g/mL in 2% glycerol prior to addition to the vaccine vial. All groups in a study received the same 1 or 5  $\mu$ g dose of carrier based on MALDI determined molecular weights, and bicinchoninic acid (BCA) assay determined concentrations.

An alum adsorption experiment was conducted at 5 $\times$  concentration to detect low concentrations of vaccine components but otherwise formulated as above. After mixing, all formulations were centrifuged at 10,000g for 20 min, and then supernatants were collected and analyzed. Protein recovery was determined using a modified Bradford assay, while UM-3006 recovery was quantified by analytical C4 RP-HPLC. For the modified Bradford assay, 50  $\mu$ L of the supernatant was plated into a 96-well plate with 150  $\mu$ L of Coomassie Plus reagent and incubated for 10 min at ambient conditions before reading at 595 nm. Experimental details and recovery values are included in Table S2. Recovery is determined by a direct comparison of average absorbance values or HPLC peak integrations between samples with and without alum as indicated.

**Animal Studies and Nociception Assays.** Vaccine Efficacy Study: BALB/c mice, both males and females, were vaccinated twice, intramuscularly (IM) in the left calf muscle 14 days apart. Experimental groups comprising 6 or 8 mice were immunized with combinations of CRM, alum, UM-3006, and/or vehicle alone as described in Table S2. Mice were sacrificed by CO<sub>2</sub> and cervical dislocation 14 days following secondary vaccination, and blood was collected from cardiac puncture.

Fentanyl Challenge Study: Female BALB/c mice were immunized with appropriate vaccine formulations at two sites in the gastrocnemius muscle on days 0, 14, and 28. Blood was collected via the facial vein on days 14, 28, and 34. Mice were challenged with 0.05 mg/kg sc fentanyl on days 21 and 35.

Animals were acclimated to the testing room for at least one hour before each challenge. Before drug administration, mice were tested for baseline antinociception on a hot plate as previously described,<sup>17</sup> and we used baseline respiratory parameters using a collar pulse oximeter as previously described.<sup>33</sup> Mice were assessed again for antinociception and respiratory depression 15 min post drug challenge. Immediately following final measurement on day 35, mice were euthanized, and trunk blood and brain were collected for analysis of fentanyl concentration using liquid chromatography-tandem mass spectrometry (LC-MS/MS) as previously described.<sup>17</sup>

**ELISA and Determination of Antibody Affinity.** F<sub>1</sub> and UM-3006 specific IgG and/or IgG subclass titers were measured via ELISA. Briefly, 96-well ELISA plates (Maxiorm, Nunc) were coated overnight at room temperature with polyclonal anti-BSA antibody (Fisher) diluted in PBS at 1:10,000. Following overnight incubation, plates were washed 3 times with phosphate buffered saline with Tween and supplied at 10 $\times$  concentration with 0.05% Tween 20 (PBST) (Seracare), blocked with 200  $\mu$ L per well Superblock (Scytek), and incubated for 1 h at 37 °C. Then, 1  $\mu$ g/mL of BSA conjugated to F<sub>1</sub> or UM-3006 was added for detection of F<sub>1</sub> or UM-3006 specific antibodies. Conjugates were incubated at 37 °C for 90 min and then washed. Serum collected from mice at either day 14, 28, or 34 post vaccination was diluted according to expected antibody concentration and serially titrated onto plates. Following incubation at 37 °C for 90 min with primary serum, plates were washed and incubated for 30 min with appropriate secondary antibody, goat-antimouse IgG-HRP, IgG2a, or IgG1 (SouthernBiotech) and developed with 100  $\mu$ L per well 3,3',5,5' tetramethylbenzidine (TMB) substrate (Seracare). Optical density was measured at 650 nm following 1 h of incubation at room temperature. Antibody titers were determined by calculating the area under the curve using XLfit software (IDBS). Serum samples with no detectable titers at a dilution of 1:25 were assigned a nominal value of 0.01 to enable graphing on a log scale.

Antibody affinity assays were performed on an Octet Red 96e instrument (ForteBio) at 30 °C with shaking at 1000 rpm in a solid black 96-well plate (Grenier). *In vivo* serum samples (analyte) and biotinylated antigen, F<sub>1</sub>-Biotin (ligand), were diluted in 10 $\times$  Kinetic Buffer (ForteBio). 10 $\times$  Kinetic Buffer was used for ligand and analyte dilutions and all subsequent steps to avoid signal variations from step to step. Assays were performed by loading F<sub>1</sub>-Biotin onto prehydrated streptavidin sensors at 0.1  $\mu$ g/mL (loading step 120s) followed by 180s baseline. Sensors were then moved into analyte to allow for association, 120s. *In vivo* serum samples were analyzed at three different dilutions; serum dilutions tested were determined based on IgG antifentanyl antibody units as determined by F<sub>1</sub> specific ELISAs. Association of the antibody to the antigen was followed by a 600 s dissociation step. Dissociation rate constants ( $k_d$ ) were calculated by processing raw data using ForteBio HT analysis software, version 11.1.3.50. All data was inspected for quality of fit to the calculated curve ( $R^2 > 0.95$ ), response between 0.25 and 3, and residual value <10% of the maximum response fitted to the curve.

**Data Analysis and Figures.** Chemical structures were produced using ChemDraw 18.2 (PerkinElmer Informatics). CRM structure was visualized using Chimera 1.14 (UCSF). GraphPad Prism 9 (GraphPad Software) was used for all statistical analyses and graphing. Soft Max Pro 6.2.1

(Molecular Devices) software was used to collect the microplate assay data. Compass for Flex Series 1.4, Flex Control 3.4, and Flex Analysis (Bruker, Daltonic) software was used to collect and analyze MALDI-ToF data. *In vivo* data were analyzed using one-way ANOVA followed by either uncorrected Fisher's least significant difference (LSD) test or Tukey's multiple comparison test, as indicated (GraphPad Prism). All data are shown as mean  $\pm$  standard error of the mean (SEM). Differences were considered significant if  $p \leq 0.05$ .

## ■ ASSOCIATED CONTENT

### SI Supporting Information

The Supporting Information is available free of charge at <https://pubs.acs.org/doi/10.1021/acs.bioconjchem.3c00347>.

Materials and instrumentation, *in vivo* comparison of F<sub>1</sub>-CRM conjugates using EDC vs EDC/NHS chemistry, table of vaccine lots, antibody affinity data, demonstration of alum adsorption, mouse challenge antibody isotype titers (PDF)

## ■ AUTHOR INFORMATION

### Corresponding Author

David Burkhart – Center for Translational Medicine, Department of Biomedical and Pharmaceutical Sciences, University of Montana, Missoula, Montana 59801, United States; Email: [david.burkhart@mso.umt.edu](mailto:david.burkhart@mso.umt.edu)

### Authors

Noah Powers – Center for Translational Medicine, Department of Biomedical and Pharmaceutical Sciences, University of Montana, Missoula, Montana 59801, United States; [orcid.org/0009-0007-6422-0220](https://orcid.org/0009-0007-6422-0220)

Casey Massena – Center for Translational Medicine, Department of Biomedical and Pharmaceutical Sciences, University of Montana, Missoula, Montana 59801, United States

Bethany Crouse – Department of Pharmacology, University of Minnesota, Minneapolis, Minnesota 55455, United States; [orcid.org/0000-0002-1984-2465](https://orcid.org/0000-0002-1984-2465)

Mira Smith – Center for Translational Medicine, Department of Biomedical and Pharmaceutical Sciences, University of Montana, Missoula, Montana 59801, United States

Linda Hicks – Center for Translational Medicine, Department of Biomedical and Pharmaceutical Sciences, University of Montana, Missoula, Montana 59801, United States

Jay T. Evans – Center for Translational Medicine, Department of Biomedical and Pharmaceutical Sciences, University of Montana, Missoula, Montana 59801, United States

Shannon Miller – Center for Translational Medicine, Department of Biomedical and Pharmaceutical Sciences, University of Montana, Missoula, Montana 59801, United States

Marco Pravetoni – Department of Psychiatry and Behavioral Sciences, University of Washington School of Medicine, Seattle, Washington 98195, United States

Complete contact information is available at: <https://pubs.acs.org/doi/10.1021/acs.bioconjchem.3c00347>

### Author Contributions

<sup>||</sup>These authors contributed equally.

## Notes

The authors declare the following competing financial interest(s): MP is the inventor and co-inventor of patents disclosing fentanyl haptens, fentanyl hapten conjugates, and methods for using them. JTE and DB are listed as inventors on patents associated with TLR7/8 ligands and their use as vaccine adjuvants. JTE and DB are also investigators at Inimmune Corporation which also researches TLR7/8 ligands and their use as OUD vaccine adjuvants.

## ■ ACKNOWLEDGMENTS

This work was supported by the National Institutes of Health through the NIH HEAL Initiative under award number 75N93020C00039 and through the National Institute on Drug Abuse under award number UG3DA048386. The work of NP and CM was supported through NIH R01 award R01AI137146-01A1. The work of BC was supported through NIDA under award number F31-DA054760. The authors would like to thank the medicinal chemistry team in the Center for Translational Medicine at the University of Montana for providing UM-3006 adjuvant. Table of contents graphic created with BioRender.com.

## ■ ABBREVIATIONS

OUD, Opioid Use Disorder; TLR, Toll-like receptor; F<sub>1</sub>, Fentanyl hapten; UM-3006, TLR7/8 agonist; CRM, Cross reactive mutant carrier antigen; MOR, mu opioid receptor; F<sub>1</sub>-CRM, Hapten conjugate; APC, antigen presenting cell; EDC, 1-ethyl-3-(3-dimethylaminopropyl)carbodiimide reagent; NHS, N-Hydroxysuccinimide; PEG, poly(ethylene glycol); MALDI-ToF, Matrix-assisted laser desorption ionization time-of-flight; F<sub>1</sub>-CRM-3006, Co-conjugate of F<sub>1</sub> hapten and UM-3006; F<sub>1</sub>-CRM+UM-3006, Admixture of hapten conjugate and UM-3006; s.c., subcutaneous

## ■ REFERENCES

- (1) Centers for Disease Control and Prevention. *Wide-ranging OnLine Data for Epidemiologic Research (WONDER)*. <https://wonder.cdc.gov/>.
- (2) Gostin, L. O.; Hodge, J. G., Jr; Noe, S. A. Reframing the Opioid Epidemic as a National Emergency. *JAMA* **2017**, *318* (16), 1539–1540.
- (3) Jones, C. M.; Einstein, E. B.; Compton, W. M. Changes in Synthetic Opioid Involvement in Drug Overdose Deaths in the United States, 2010–2016. *JAMA* **2018**, *319* (17), 1819–1821.
- (4) Ciccarone, D. Fentanyl in the US Heroin Supply: A Rapidly Changing Risk Environment. *Int. J. Drug Policy* **2017**, *46*, 107–111.
- (5) Suzuki, J.; El-Haddad, S. A Review: Fentanyl and Non-Pharmaceutical Fentanyls. *Drug Alcohol Depend.* **2017**, *171*, 107–116.
- (6) National Academies of Sciences, Engineering, and Medicine; Health and Medicine Division; Board on Health Sciences Policy; Disorder, Committee on Medication-Assisted Treatment for Opioid Use Disorder. The Effectiveness of Medication-Based Treatment for Opioid Use Disorder. In *Medications for Opioid Use Disorder Save Lives*; Mancher, M., Leshner, A. I., Eds.; National Academies Press (US), 2019. <https://www.ncbi.nlm.nih.gov/books/NBK541393/>
- (7) Obadia, Y.; Perrin, V.; Feroni, I.; Vlahov, D.; Moatti, J.-P. Injecting Misuse of Buprenorphine among French Drug Users. *Addiction* **2001**, *96* (2), 267–272.
- (8) Alho, H.; Sinclair, D.; Vuori, E.; Holopainen, A. Abuse Liability of Buprenorphine–Naloxone Tablets in Untreated IV Drug Users. *Drug Alcohol Depend.* **2007**, *88* (1), 75–78.
- (9) Volkow, N. D.; Blanco, C. The Changing Opioid Crisis: Development, Challenges and Opportunities. *Mol. Psychiatry* **2021**, *26* (1), 218–233.

- (10) Bell, J.; Strang, J. Medication Treatment of Opioid Use Disorder. *Biol. Psychiatry* **2020**, *87* (1), 82–88.
- (11) Lim, J.; Farhat, I.; Douros, A.; Panagiotoglou, D. Relative Effectiveness of Medications for Opioid-Related Disorders: A Systematic Review and Network Meta-Analysis of Randomized Controlled Trials. *PLoS One* **2022**, *17* (3), No. e0266142.
- (12) Pravetoni, M.; Comer, S. D. Development of Vaccines to Treat Opioid Use Disorders and Reduce Incidence of Overdose. *Neuropharmacology* **2019**, *158*, No. 107662.
- (13) Rzasla Lynn, R.; Galinkin, J. Naloxone Dosage for Opioid Reversal: Current Evidence and Clinical Implications. *Ther. Adv. Drug Saf.* **2018**, *9* (1), 63–88.
- (14) Torralva, R.; Janowsky, A. Noradrenergic Mechanisms in Fentanyl-Mediated Rapid Death Explain Failure of Naloxone in the Opioid Crisis. *J. Pharmacol. Exp. Ther.* **2019**, *371* (2), 453–475.
- (15) Kelly, E.; Sutcliffe, K.; Cavallo, D.; Ramos-Gonzalez, N.; Alhosan, N.; Henderson, G. The Anomalous Pharmacology of Fentanyl. *Br. J. Pharmacol.* **2023**, *180* (7), 797–812.
- (16) Pergolizzi, J. V., Jr; Webster, L. R.; Vortsman, E.; Ann LeQuang, J.; Raffa, R. B. Wooden Chest Syndrome: The Atypical Pharmacology of Fentanyl Overdose. *J. Clin. Pharm. Ther.* **2021**, *46* (6), 1505–1508.
- (17) Robinson, C.; Gradinati, V.; Hamid, F.; Baehr, C.; Crouse, B.; Averick, S.; Kovaliov, M.; Harris, D.; Runyon, S.; Baruffaldi, F.; LeSage, M.; Comer, S.; Pravetoni, M. Therapeutic and Prophylactic Vaccines to Counteract Fentanyl Use Disorders and Toxicity. *J. Med. Chem.* **2020**, *63* (23), 14647–14667.
- (18) Han, Y.; Cao, L.; Yuan, K.; Shi, J.; Yan, W.; Lu, L. Unique Pharmacology, Brain Dysfunction, and Therapeutic Advancements for Fentanyl Misuse and Abuse. *Neurosci. Bull.* **2022**, *38*, 1365–1382.
- (19) Townsend, E. A.; Banks, M. L. Preclinical Evaluation of Vaccines to Treat Opioid Use Disorders: How Close Are We to a Clinically Viable Therapeutic? *CNS Drugs* **2020**, *34* (5), 449–461.
- (20) Xu, A.; Kosten, T. R. Current Status of Immunotherapies for Addiction. *Ann. N.Y. Acad. Sci.* **2021**, *1489* (1), 3–16.
- (21) Pravetoni, M.; Comer, S. D. Development of Vaccines to Treat Opioid Use Disorders and Reduce Incidence of Overdose. *Neuropharmacology* **2019**, *158*, No. 107662.
- (22) Miller, S. M.; Crouse, B.; Hicks, L.; Amin, H.; Cole, S.; Bazin, H. G.; Burkhart, D. J.; Pravetoni, M.; Evans, J. T. A Lipidated TLR7/8 Adjuvant Enhances the Efficacy of a Vaccine against Fentanyl in Mice. *Npj Vaccines* **2023**, *8* (1), 1–14.
- (23) Barrientos, R. C.; Whalen, C.; Torres, O. B.; Sulima, A.; Bow, E. W.; Komla, E.; Beck, Z.; Jacobson, A. E.; Rice, K. C.; Matyas, G. R. Bivalent Conjugate Vaccine Induces Dual Immunogenic Response That Attenuates Heroin and Fentanyl Effects in Mice. *Bioconjugate Chem.* **2021**, *32* (11), 2295–2306.
- (24) Baehr, C.; Robinson, C.; Kassick, A.; Jahan, R.; Gradinati, V.; Averick, S. E.; Runyon, S. P.; Pravetoni, M. Preclinical Efficacy and Selectivity of Vaccines Targeting Fentanyl, Alfentanil, Sufentanil, and Acetylfentanyl in Rats. *ACS Omega* **2022**, *7* (19), 16584–16592.
- (25) Cornuz, J.; Zwahlen, S.; Jungi, W. F.; Osterwalder, J.; Klingler, K.; van Melle, G.; Bangala, Y.; Guessous, I.; Muller, P.; Willers, J.; Maurer, P.; Bachmann, M. F.; Cerny, T. A Vaccine against Nicotine for Smoking Cessation: A Randomized Controlled Trial. *PLoS One* **2008**, *3* (6), No. e2547.
- (26) Hatsukami, D. K.; Jorenby, D. E.; Gonzales, D.; Rigotti, N. A.; Glover, E. D.; Oncken, C. A.; Tashkin, D. P.; Reus, V. I.; Akhavan, R. C.; Fahim, R. E. F.; Kessler, P. D.; Niknian, M.; Kalnik, M. W.; Rennard, S. I. Immunogenicity and Smoking Cessation Outcomes for a Novel Nicotine Immunotherapeutic. *Clin. Pharmacol. Ther.* **2011**, *89* (3), 392–399.
- (27) Martell, B. A.; Orson, F. M.; Poling, J.; Mitchell, E.; Rossen, R. D.; Gardner, T.; Kosten, T. R. Cocaine Vaccine for the Treatment of Cocaine Dependence in Methadone Maintained Patients: A Randomized Double-Blind Placebo-Controlled Efficacy Trial. *Arch. Gen. Psychiatry* **2009**, *66* (10), 1116–1123.
- (28) Alving, C. R.; Matyas, G. R.; Torres, O.; Jalah, R.; Beck, Z. Adjuvants for Vaccines to Drugs of Abuse and Addiction. *Vaccine* **2014**, *32* (42), 5382–5389.
- (29) Bremer, P. T.; Schlosburg, J. E.; Lively, J. M.; Janda, K. D. Injection Route and TLR9 Agonist Addition Significantly Impact Heroin Vaccine Efficacy. *Mol. Pharmaceutics* **2014**, *11* (3), 1075–1080.
- (30) Hwang, C. S.; Bremer, P. T.; Wenthur, C. J.; Ho, S. O.; Chiang, S.; Ellis, B.; Zhou, B.; Fujii, G.; Janda, K. D. Enhancing Efficacy and Stability of an Antiheroine Vaccine: Examination of Antinociception, Opioid Binding Profile, and Lethality. *Mol. Pharmaceutics* **2018**, *15* (3), 1062–1072.
- (31) Pravetoni, M.; Vervacke, J. S.; Distefano, M. D.; Tucker, A. M.; Laudenbach, M.; Pentel, P. R. Effect of Currently Approved Carriers and Adjuvants on the Pre-Clinical Efficacy of a Conjugate Vaccine against Oxycodone in Mice and Rats. *PLoS One* **2014**, *9* (5), No. e96547.
- (32) Matyas, G. R.; Mayorov, A. V.; Rice, K. C.; Jacobson, A. E.; Cheng, K.; Iyer, M. R.; Li, F.; Beck, Z.; Janda, K. D.; Alving, C. R. Liposomes Containing Monophosphoryl Lipid A: A Potent Adjuvant System for Inducing Antibodies to Heroin Hapten Analogs. *Vaccine* **2013**, *31* (26), 2804–2810.
- (33) Laudenbach, M.; Baruffaldi, F.; Robinson, C.; Carter, P.; Seelig, D.; Baehr, C.; Pravetoni, M. Blocking Interleukin-4 Enhances Efficacy of Vaccines for Treatment of Opioid Abuse and Prevention of Opioid Overdose. *Sci. Rep.* **2018**, *8* (1), No. 5508.
- (34) Miller, S. M.; Cybulski, V.; Whitacre, M.; Bess, L. S.; Livesay, M. T.; Walsh, L.; Burkhart, D.; Bazin, H. G.; Evans, J. T. Novel Lipidated Imidazoquinoline TLR7/8 Adjuvants Elicit Influenza-Specific Th1 Immune Responses and Protect Against Heterologous H3N2 Influenza Challenge in Mice. *Front. Immunol.* **2020**, *11*. DOI: 10.3389/fimmu.2020.00406
- (35) Lynn, G. M.; Laga, R.; Darrach, P. A.; Ishizuka, A. S.; Balaci, A. J.; Dulcey, A. E.; Pechar, M.; Pola, R.; Gerner, M. Y.; Yamamoto, A.; Buechler, C. R.; Quinn, K. M.; Smelkinson, M. G.; Vanek, O.; Cawood, R.; Hills, T.; Vasalatiy, O.; Kastenmuller, K.; Francica, J. R.; Stutts, L.; Tom, J. K.; Ryu, K. A.; Esser-Kahn, A. P.; Etrych, T.; Fisher, K. D.; Seymour, L. W.; Seder, R. A. In Vivo Characterization of the Physicochemical Properties of TLR Agonist Delivery That Enhance Vaccine Immunogenicity. *Nat. Biotechnol.* **2015**, *33* (11), 1201–1210.
- (36) Holbrook, B. C.; Kim, J. R.; Blevins, L. K.; Jorgensen, M. J.; Kock, N. D.; D'Agostino, R. B., Jr.; Aycock, S. T.; Hadimani, M. B.; King, S. B.; Parks, G. D.; Alexander-Miller, M. A. A Novel R848-Conjugated Inactivated Influenza Virus Vaccine Is Efficacious and Safe in a Neonate Nonhuman Primate Model. *J. Immunol.* **2016**, *197* (2), 555–564.
- (37) Dowling, D. J. Recent Advances in the Discovery and Delivery of TLR7/8 Agonists as Vaccine Adjuvants. *ImmunoHorizons* **2018**, *2* (6), 185–197.
- (38) Pockros, P. J.; Guyader, D.; Patton, H.; Tong, M. J.; Wright, T.; McHutchison, J. G.; Meng, T.-C. Oral Resiquimod in Chronic HCV Infection: Safety and Efficacy in 2 Placebo-Controlled, Double-Blind Phase IIa Studies. *J. Hepatol.* **2007**, *47* (2), 174–182.
- (39) Smirnov, D.; Schmidt, J. J.; Capecchi, J. T.; Wightman, P. D. Vaccine Adjuvant Activity of 3M-052: An Imidazoquinoline Designed for Local Activity without Systemic Cytokine Induction. *Vaccine* **2011**, *29* (33), 5434–5442.
- (40) Buonsanti, C.; Balocchi, C.; Harfouche, C.; Corrente, F.; Galli Stampino, L.; Mancini, F.; Tontini, M.; Malyala, P.; Bufali, S.; Baudner, B.; De Gregorio, E.; Valiante, N. M.; O'Hagan, D. T.; Rappuoli, R.; D'Oro, U. Novel Adjuvant Alum-TLR7 Significantly Potentiates Immune Response to Glycoconjugate Vaccines. *Sci. Rep.* **2016**, *6* (1), No. 29063.
- (41) Cortez, A.; Li, Y.; Miller, A. T.; Zhang, X.; Yue, K.; Maginnis, J.; Hampton, J.; Hall, D. S.; Shapiro, M.; Nayak, B.; D'Oro, U.; Li, C.; Skibinski, D.; Mbow, M. L.; Singh, M.; O'Hagan, D. T.; Cooke, M. P.; Valiante, N. M.; Wu, T. Y.-H. Incorporation of Phosphonate into Benzonaphthridine Toll-like Receptor 7 Agonists for Adsorption to Aluminum Hydroxide. *J. Med. Chem.* **2016**, *59* (12), 5868–5878.

- (42) Gunzer, M.; Riemann, H.; Basoglu, Y.; Hillmer, A.; Weishaupt, C.; Balkow, S.; Benninghoff, B.; Ernst, B.; Steinert, M.; Scholzen, T.; Sunderkötter, C.; Grabbe, S. Systemic Administration of a TLR7 Ligand Leads to Transient Immune Incompetence Due to Peripheral-Blood Leukocyte Depletion. *Blood* **2005**, *106* (7), 2424–2432.
- (43) Wille-Reece, U.; Flynn, B. J.; Loré, K.; Koup, R. A.; Kedl, R. M.; Mattapallil, J. J.; Weiss, W. R.; Roederer, M.; Seder, R. A. HIV Gag Protein Conjugated to a Toll-like Receptor 7/8 Agonist Improves the Magnitude and Quality of Th1 and CD8+ T Cell Responses in Nonhuman Primates. *Proc. Natl. Acad. Sci. U. S. A.* **2005**, *102* (42), 15190–15194.
- (44) Massena, C. J.; Lathrop, S. K.; Davison, C. J.; Schoener, R.; Bazin, H. G.; Evans, J. T.; Burkhart, D. J. A Tractable Covalent Linker Strategy for the Production of Immunogenic Antigen-TLR7/8L Bioconjugates. *Chem. Commun.* **2021**, *57* (38), 4698–4701.
- (45) Donadei, A.; Balocchi, C.; Mancini, F.; Proietti, D.; Gallorini, S.; O'Hagan, D. T.; D'Oro, U.; Berti, F.; Baudner, B. C.; Adamo, R. The Adjuvant Effect of TLR7 Agonist Conjugated to a Meningococcal Serogroup C Glycoconjugate Vaccine. *Eur. J. Pharm. Biopharm. Off. J. Arbeitsgemeinschaft Pharm. Verfahrenstechnik EV* **2016**, *107*, 110–119.
- (46) Du, J.-J.; Wang, C.-W.; Xu, W.-B.; Zhang, L.; Tang, Y.-K.; Zhou, S.-H.; Gao, X.-F.; Yang, G.-F.; Guo, J. Multifunctional Protein Conjugates with Built-in Adjuvant (Adjuvant-Protein-Antigen) as Cancer Vaccines Boost Potent Immune Responses. *iScience* **2020**, *23* (3), No. 100935.
- (47) Yang, Y. Side Reactions Upon Amino Acid/Peptide Carboxyl Activation. In *Side Reactions in Peptide Synthesis*; Yang, Y., Ed.; Academic Press: Oxford, UK, 2016; pp 95–118. DOI: 10.1016/B978-0-12-801009-9.00005-7.
- (48) *PEGylated Protein Drugs: Basic Science and Clinical Applications*; Veronese, F. M., Ed.; Milestones in Drug Therapy Book Series; Birkhäuser: Basel, Switzerland, 2009.
- (49) Zheng, C. Y.; Ma, G.; Su, Z. Native PAGE Eliminates the Problem of PEG–SDS Interaction in SDS-PAGE and Provides an Alternative to HPLC in Characterization of Protein PEGylation. *ELECTROPHORESIS* **2007**, *28* (16), 2801–2807.
- (50) Snapper, C. M.; Paul, W. E. Interferon- $\gamma$  and B Cell Stimulatory Factor-1 Reciprocally Regulate Ig Isotype Production. *Science* **1987**, *236* (4804), 944–947.
- (51) Germann, T.; Gately, M. K.; Schoenhaut, D. S.; Lohoff, M.; Mattner, F.; Fischer, S.; Jin, S.-C.; Schmitt, E.; Rüde, E. Interleukin-12/T Cell Stimulating Factor, a Cytokine with Multiple Effects on T Helper Type 1 (Th1) but Not on Th2 Cells. *Eur. J. Immunol.* **1993**, *23* (8), 1762–1770.
- (52) Stevens, T. L.; Bossie, A.; Sanders, V. M.; Fernandez-Botran, R.; Coffman, R. L.; Mosmann, T. R.; Vitetta, E. S. Regulation of Antibody Isotype Secretion by Subsets of Antigen-Specific Helper T Cells. *Nature* **1988**, *334* (6179), 255–258.
- (53) Marrack, P.; McKee, A. S.; Munks, M. W. Towards an Understanding of the Adjuvant Action of Aluminium. *Nat. Rev. Immunol.* **2009**, *9* (4), 287–293.
- (54) Baehr, C.; Kelcher, A. H.; Khaimraj, A.; Reed, D. E.; Pandit, S. G.; AuCoin, D.; Averick, S.; Pravetoni, M. Monoclonal Antibodies Counteract Opioid-Induced Behavioral and Toxic Effects in Mice and Rats. *J. Pharmacol. Exp. Ther.* **2020**, *375* (3), 469–477.
- (55) Kastenmüller, K.; Wille-Reece, U.; Lindsay, R. W. B.; Trager, L. R.; Darrah, P. A.; Flynn, B. J.; Becker, M. R.; Udey, M. C.; Clausen, B. E.; Igyarto, B. Z.; Kaplan, D. H.; Kastenmüller, W.; Germain, R. N.; Seder, R. A. Protective T Cell Immunity in Mice Following Protein-TLR7/8 Agonist-Conjugate Immunization Requires Aggregation, Type I IFN, and Multiple DC Subsets. *J. Clin. Invest.* **2011**, *121* (5), 1782–1796.
- (56) Raleigh, M. D.; Baruffaldi, F.; Peterson, S. J.; Le Naour, M.; Harmon, T. M.; Vigliaturo, J. R.; Pentel, P. R.; Pravetoni, M. A Fentanyl Vaccine Alters Fentanyl Distribution and Protects against Fentanyl-Induced Effects in Mice and Rats. *J. Pharmacol. Exp. Ther.* **2019**, *368* (2), 282–291.
- (57) Barrientos, R. C.; Bow, E. W.; Whalen, C.; Torres, O. B.; Sulima, A.; Beck, Z.; Jacobson, A. E.; Rice, K. C.; Matyas, G. R. Novel Vaccine That Blunts Fentanyl Effects and Sequesters Ultrapotent Fentanyl Analogues. *Mol. Pharmaceutics* **2020**, *17* (9), 3447–3460.
- (58) Townsend, E. A.; Bremer, P. T.; Faunce, K. E.; Negus, S. S.; Jaster, A. M.; Robinson, H. L.; Janda, K. D.; Banks, M. L. Evaluation of a Dual Fentanyl/Heroin Vaccine on the Antinociceptive and Reinforcing Effects of a Fentanyl/Heroin Mixture in Male and Female Rats. *ACS Chem. Neurosci.* **2020**, *11* (9), 1300–1310.
- (59) Zhou, S.-H.; Li, Y.-T.; Zhang, R.-Y.; Liu, Y.-L.; You, Z.-W.; Bian, M.-M.; Wen, Y.; Wang, J.; Du, J.-J.; Guo, J. Alum Adjuvant and Built-in TLR7 Agonist Synergistically Enhance Anti-MUC1 Immune Responses for Cancer Vaccine. *Front. Immunol.* **2022**, *13*, No. 857779.
- (60) Huseby Kelcher, A. M.; Baehr, C. A.; Hamid, F. A.; Hart, G. T.; Pravetoni, M. Contribution of Antibody-Mediated Effector Functions to the Mechanism of Efficacy of Vaccines for Opioid Use Disorders. *J. Immunol.* **2021**, *207* (3), 860–867.